Desalination and Water Treatment
www.deswater.com

doi:10.5004/dwt.2019.24624

166 (2019) 83–91
October

Treatment of Reactive Red 241 dye by electro coagulation/biosorption coupled process in a new hybrid reactor

Farhan Javed[a,*], Nadeem Feroze[b], Naveed Ramzan[b], Amir Ikhlaq[c], Mohsin Kazmi[d], Hafiz Muhammad Shahzad Munir[b]

[a]*University of Engineering and Technology, Department of Chemical Engineering, Lahore, FSD Campus, Pakistan, Tel. +92412433508, email: farhan.javed@uet.edu.pk (F. Javed)*
[b]*University of Engineering and Technology, Department of Chemical Engineering, Lahore, Pakistan, email: drnchohan@yahoo.com (N. Feroze), drnramzan@uet.edu.pk (N. Ramzan), engrsm124@gmail.com (H.M.S. Munir)*
[c]*University of Engineering and Technology, Institute of Environmental Engineering and Research, Lahore, Pakistan, email: aamirikhlaq@uet.edu.pk (A. Ikhlaq)*
[d]*University of Engineering and Technology, Department of Chemical Engineering, Lahore, KSK Campus, Pakistan, email: engr.smalikazmi@gmail.com (M. Kazmi)*

Received 23 January 2019; Accepted 26 June 2019

ABSTRACT

The current research evaluates the treatment of Reactive Red 241, an anionic textile dye, by electro coagulation/biosorption (EC/BS) coupled process in a new hybrid reactor. The composite biomass pellets, suspended in the reactor using a twin rotary bucket system, were exploited as biosorbent. The influencing operational parameters of current density, pH, biosorbent dosage, and initial dye concentration were elucidated for decolorization. An effective performance of hybrid reactor resulted in complete decolorization with lower energy requirement and operational cost. At optimum conditions, color removal efficiency of 99.56% was obtained after 20 min at current density 21.7 mA/cm^2, pH 7, biosorbent dosage 8 g/L, and dye concentration 50 mg/L with specific electrical energy consumption of 1.7 kWh/kg dye, and operational cost of 0.307 $/kg dye. The results indicate the potential of electro coagulation/biosorption (EC/BS) coupled hybrid reactor for the effective treatment of colored effluents.

Keywords: Hybrid reactor; Electro coagulation; Biosorption; Biomass composite pellet, Reactive red 241.

1. Introduction

Colored wastewater discharged from textile industries causes severe contamination of the water resources and poses a hazard to the environment [1] as it carries assorted dyes, suspended and dissolved solids, a high concentration of salts and various auxiliary chemicals [2]. Dyes are the main pollutant in textile wastewater that is detrimental to the life by causing various toxic and mutagenic effects and have low biodegradability owing to the conjugated ring type structure that imparts recalcitrant nature [3]. Dye treatment in aqueous solution using various techniques have been studied such as adsorption [4], membrane process [2], advanced oxidation process [5], the biological process [6], flocculation [7], coagulation [8] and electrochemical method [9]. However, a continuous research is on the development of cost-effective, faster and efficient treatment method for industrial wastewater containing a diversity of pollutants.

Electro coagulation (EC) has emerged as an efficient electrochemical method for the treatment of dyes [10]. The numerous advantages of EC over other techniques include the elimination of the use of chemicals, low investment requirement, compact equipment requiring a small area, lesser sludge generation, eco-friendly operation and no sec-

*Corresponding author.

ondary pollutants formation [11]. EC utilizes electrons as reagents for the in-situ generation of the coagulants from sacrificial metal electrodes by passing the current. EC utilizing the aluminum metal electrodes involves the following chemical reactions [12].

Oxidation at the anode: $Al_{(s)} \rightarrow Al^{3+} + 3e^{-}$ (1)

Reduction at the cathode: $3H_2O + 3e^{-} \rightarrow \frac{3}{2}H_{2(g)} + 3OH^{-}$ (2)

The bulk of the solution:

$$Al^{3+} + 3H_2O \rightarrow Al(OH)_{3(s)} + \frac{3}{2}H_{2(g)} \quad (3)$$

Dye interaction:

$$Dye + MonomericAlspecies \rightarrow \left[Dye - monomericAl\right]_{(s)} \quad (4)$$

$$Dye + PolymericAlspecies \rightarrow \left[Dye - PolymericAl\right]_{(s)} \quad (5)$$

$$Dye + Al(OH)_{3(s)} \rightarrow \left[particle\right] \quad (6)$$

Polymerization: $nAl(OH)_{3(s)} \rightarrow Al_n(OH)_{3n(s)}$ (7)

The aluminum cations released at the anode undergo the chemical reaction with hydroxyl ions from the cathode to form amorphous $Al(OH)_3$ flocs. Numerous monomeric and the polymeric hydroxide aluminum species are formed in the bulk of solution depending upon the prevailing pH that provides large surface area due to the gelatinous surface and causes dye entrapment by precipitation, coagulation and adsorption mechanisms [13]. Moreover, a high concentration of electrolytes such as NaCl, Na_2SO_4, Na_2CO_3 in real textile dye bath effluents provides an inherent superiority to the application of EC treatment [14]. The NaCl acting as electrolyte not only reduces the voltage requirement for the E-C process by increasing electric conductivity but also generates strong oxidizing agents such as Cl_2, hypochlorous acid, and OCl^- that readily destroys the organic pollutants present in wastewater [15].

$$Cl^{-} \rightarrow Cl_2 + 2e^{-} \quad (8)$$

$$Cl_2 + H_2O \rightarrow HOCl + H^{+} + Cl^{-} \quad (9)$$

$$HOCl \rightarrow H^{+} + OCl^{-} \quad (10)$$

Biosorption (BS) of textile dyes onto various lignocellulosic biosorbents such as roots [16], peanut shell [17], leaves [4], bagasse [18] and sawdust [19] with high removal efficiencies makes it a non-toxic, eco-friendly and economical technique due to abundance availability, renew ability, and biodegradability of these materials. The application of pollutant adsorption on an industrial scale has certain intrinsic drawbacks when adsorbents are utilized in powdered forms such as time-consuming solid-liquid disengagement step required after treatment, the risk of clogging and the high cost of separation [20,21]. The pelletized adsorbents offer various advantages like easy separation after treatment, good mechanical properties, easy stabilization and lesser clogging risk [20–22]. Due to diverse pollutants in real textile industry effluents, the application of a single treatment method has certain limitations while the hybrid techniques have proved to be more efficient, feasible and require compact reactors reducing the capital cost requirements [23–25].

In current research, treatment of Reactive Red 241 (RR-241), an anionic textile dye, by electro coagulation/biosorption (EC/BS) coupled process in a new hybrid reactor was performed. The composite biomass pellets prepared from a mixture of two biosorbents of Sapindus Mukorossi dead leaves powder (DLP) and powder micro crystalline cellulose (MCL), were exploited as biosorbent and suspended in the reactor using a twin rotary bucket system. To the author's knowledge, the current study is the first report on the application of novel Sapindus Mukorossi dead leaves based pelletized biosorbent with electro coagulation hybrid process. Moreover, the new reactor geometry containing the rotary buckets (not present in conventional EC reactors) was studied with the biosorbent pellets suspended in the solution. The color abatement was examined as a function of influencing operational parameters of current density, pH, biosorbent dosage, and initial dye concentration. The kinetic study, specific electrical energy consumption, unit electrode consumption and operational cost were evaluated.

2. Materials and methods

2.1. Chemicals

The textile dye [Reactive Red 241] used in the current study was obtained from Archroma (Switzerland) and used without any further purification. The analytical grade chemicals Sodium chloride, HCl, and NaOH were procured from Sigma-Aldrich (USA). The chemical structure with properties of the dye is shown in Fig. 1. Micro crystalline cellulose was obtained from FMC Biopolymers (USA). The dead leaves of Sapindus Mukorossi were gathered from the vicinity of the local trees.

2.2. Biomass composite pellets preparation

The two biosorbent materials of Sapindus Mukorossi dead leaves powder (DLP) and powder micro crystalline cellulose (MCL) were used to prepare the biomass composite pellets. The dead leaves collected from the vicinity of the local trees were washed several times to remove all dirt and extraneous materials until pH of wash water was neutralized. The moisture of leaves was removed by air drying at room temperature and then oven drying at a temperature of 60°C for 24 h. The leaves were then ground and sieved

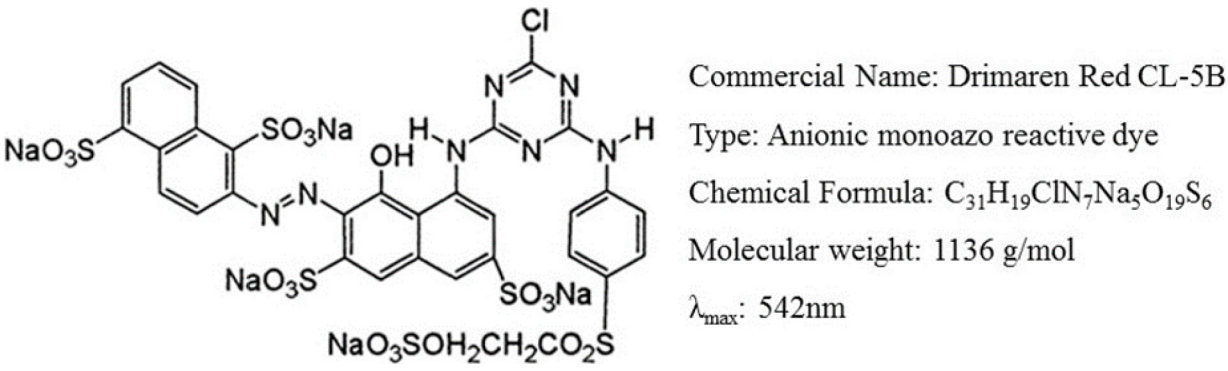

Fig. 1. RR-241 dye structure and properties.

through 70 mesh sieves to obtain Sapindus Mukorossi dead leaves powder (DLP). The micro crystalline cellulose (MCL) was used as received with an average particle size of 200 µm. A formulation was prepared by mixing the DLP and MCL in a weight ratio of (1:1) and ultra-pure deionized water was then added 20% by weight as a mass wetting agent. The wet biomass was converted into pellets using a locally made pellet mill by an extrusion process. The obtained pellets were dried at 60°C in the oven for 6 h and stored in airtight containers.

2.3. Hybrid reactor setup

The hybrid reactor setup shown in Fig. 2, consists of a Pyrex glass rectangular tank having a capacity up to 4 L with dimensions of 21 cm (length) * 10.2 cm (width) * 19 cm (height). Two flat rectangular aluminum plate electrodes were mounted vertically in the reactor and set 2 cm apart parallel to each other. The effective submerged electrode area was 48.39 cm^2. The electrode plates were attached to a local made DC power supply (LPS 6030) as a current generator. Air was dispersed into the reactor for flotation and mixing purpose by two porous spargers at the bottom of the reactor. Two closed cylindrical perforated rotary buckets made of plexi glass having 3.4 cm (diameter) and 7.8 cm (length) each, were suspended in the reactor to hold the biomass composite pellets. The rotary buckets were connected to the rpm control box through coupling rods with interconnected dual motor assembly to assign the same rpm at a single time in a clockwise direction.

2.4 Experimental and analytical methods

The synthetic colored wastewater was produced by dissolving the specific amount of RR-241 in distilled water. The batch experimental runs were performed by taking 2 L of colored wastewater at room temperature. For each run, 2 g/L of NaCl electrolyte was added. The initial pH was set by aliquots of 1 M NaOH or 1 M HCl to the desired value by pH meter (Model Hanna HI9811-5). The twin rotary buckets were loaded with the desired amount of biosorbent pellets at the start of each run and the bucket rpm were set. The applied current density was set by a DC power supply. Before each run, the electrodes were first cleaned by washing with dilute HCl along with the surface rubbing using fine grade emery paper and then washed with ultra pure

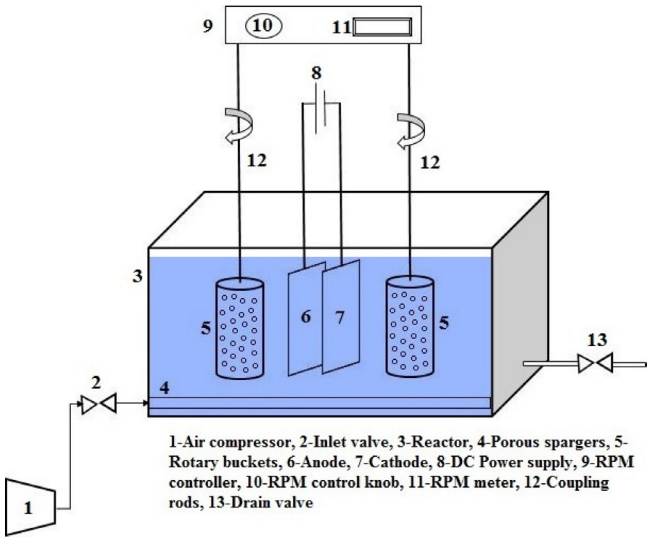

Fig. 2. Hybrid reactor setup.

deionized water and used after drying [29]. For each experimental run, the samples taken at fixed time intervals were filtered and analyzed for absorbance by UV-Vis spectrophotometer (Perkin Elmer Lambda 35). The decolorization efficiency were determined by equation:

$$Y_{COL}(\%) = \frac{C_1 - C_2}{C_1} \tag{11}$$

where C_1 and C_2 correspond to the initial and final concentrations (mg/L). The specific electrical energy consumption (SEEC-kWh/Kg dye) in hybrid reactor for treatment of RR-241 by the equation [26].

$$SEEC = \frac{U \cdot I \cdot t}{1000 \cdot V \cdot C_1 \cdot \frac{Y_t}{100}} \tag{12}$$

where U is applied voltage (V), I is current intensity (A), t is time (h), V is solution volume (m^3), Y_t is the decolorization efficiency. The unit electrode material consumption (UMC-kg/kg dye) was determined by the equation [26].

$$UMC = \frac{A \cdot I \cdot t}{n \cdot F \cdot V \cdot C_1 \cdot \frac{Y_t}{100}} \tag{13}$$

where A is the atomic weight of aluminum (26.98 g/mol), (n = 3) is the number of electrons transferred, and F is Faraday's constant (96487 C/mol) respectively.

2.5. Characterization techniques

The functional groups at the surface of biosorbent pellets were characterized by (FTIR) Fourier transform infrared spectrometer (Bruker, Alpha-E) among 500–4000 cm^{-1} range. The texture at surface and morphology of biosorbent pellets along with elemental analysis were characterized by scanning electron microscope (SEM) linked with an (EDX) energy dispersive X-ray spectrometer (Tescan, Vega LMU). The specific surface area of biosorbent pellets, pore size, and pore volume were determined by Brunauer-Emmett-Teller (BET) surface area and pore size analyzer (Quantachrome, NOVA1200e).

The flocks generated by the EC in solution were collected and dried in an oven at 105°C for several hours to remove all the moisture and then converted to powder form by mortar and pestle. The functional groups associated with the flocks were identified by FTIR spectrometer (Bruker, Alpha-E) among 500–4000 cm^{-1} range. The visual surface morphology of flocks was characterized by SEM-EDX spectrometer (Tescan, Vega LMU).

3. Results and discussion

3.1. Characterization results

The FTIR of unloaded and dye-loaded biosorbent pellets exhibiting characteristics peaks among 500–4000 cm^{-1} wavelength range is given in Fig. 3(a). The sharp peaks obtained at 1119.81 cm^{-1}, 1056.35 cm^{-1} and 987.74 cm^{-1} are the characteristics of a C-O stretch of carboxylic acid and C-N, N-H vibrations of amine [26,27]. The peaks at 3280.44 cm^{-1} and 3286.54 cm^{-1} correspond to the O-H stretch of the hydroxyl group and water adsorbed. The peaks at 1643.47 cm^{-1} and 1644.07 cm^{-1} are characteristics of stretching vibrations of C=O carbonyl group. The peaks in the lower region at 868.93 cm^{-1}, 783.96 cm^{-1} and 653.80 cm^{-1} represents C-H bending [26,27]. The drift in the peaks confirms the presence of RR-241 molecules on the biosorbent pellets surface.

The SEM-EDX images of unloaded and dye-loaded biosorbent pellets are shown in Fig. 4 (a, b). The unloaded condition SEM image (Fig. 4a) indicates the porous irregular surface of biosorbent pellets and dye-loaded SEM image (Fig. 4b) shows the pore coverage by the dye molecules. The EDX peaks revealed the presence of main elements of C, O, P and Ca. The increase in weight % of C from 13.26% to 25.81% was observed after dye loading (Table 1).

The determined results of the (BET) analysis of biosorbent pellets exhibited the specific surface area of 13.18 m^2/g, the average pore diameter of 46.72°A and total pore volume of 3.41×10^{-2} cm^3/g.

The FTIR spectrum of unloaded and dye-loaded Al flocks in 500–4000 cm^{-1} wavelength region is shown in Fig. 3b. The broad peaks observed at 3331.27 cm^{-1} and 3315.32 cm^{-1} correspond to the O-H stretch vibrations of $Al(OH)_3$ formed in the solution [13,28]. The sharp peaks at 1637.49 cm^{-1} and 1636.38 cm^{-1} indicate H-O-H stretching vibrations. The peaks at 1066.7 cm^{-1} represent the Al-O-H stretching vibrations of Al flocks [13,28]. The peaks at 668.76 cm^{-1} and 727.63 cm^{-1} correspond to the Al-O stretching [13,28]. The drift in the peaks owing to the O-H and N-H stretching of dye molecules confirms the dye removal mechanism by Al flocks [28].

Figs. 4c, d show the SEM-EDX images of unloaded and dye-loaded Al flocks. The unloaded SEM image (Fig. 4c) revealed an amorphous, porous and gelatinous texture of the surface. A smoother surface was observed (Fig. 4d) after the dye loading. The EDX peaks showed the presence of elements of Al, O, C, Cl, and Na. The elemental composition is shown in Table 1. Similar results have been reported [13, 28].

3.2. Comparison of processes

The RR-241 decolorization was studied as function of different processes (BS, EC, EC/BS). The experimental results

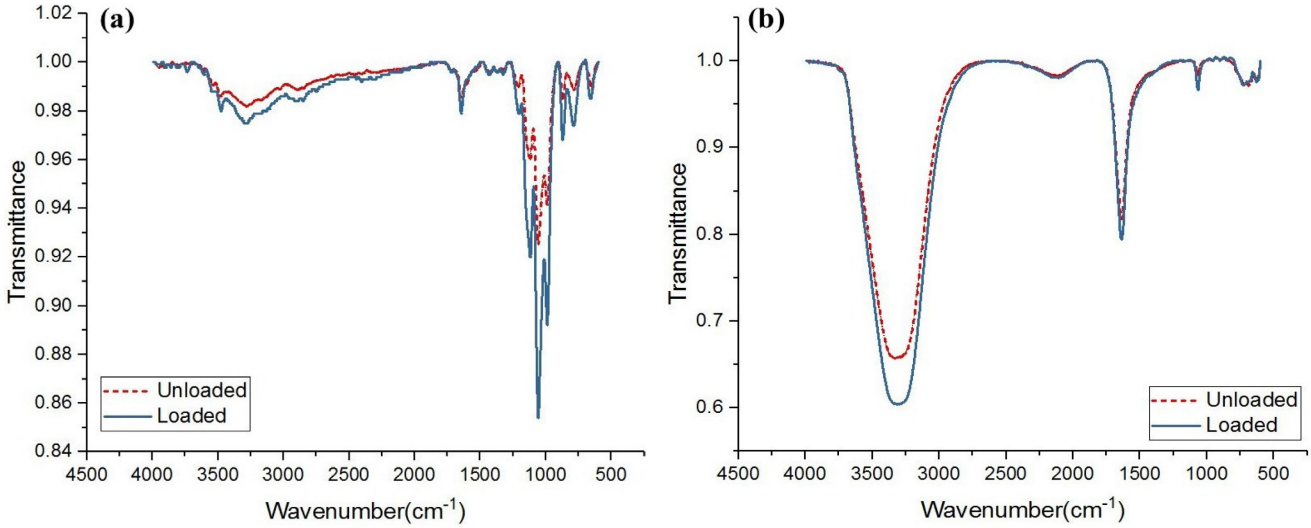

Fig. 3. FTIR of (a) Biomass pellets (b) Al Flocks.

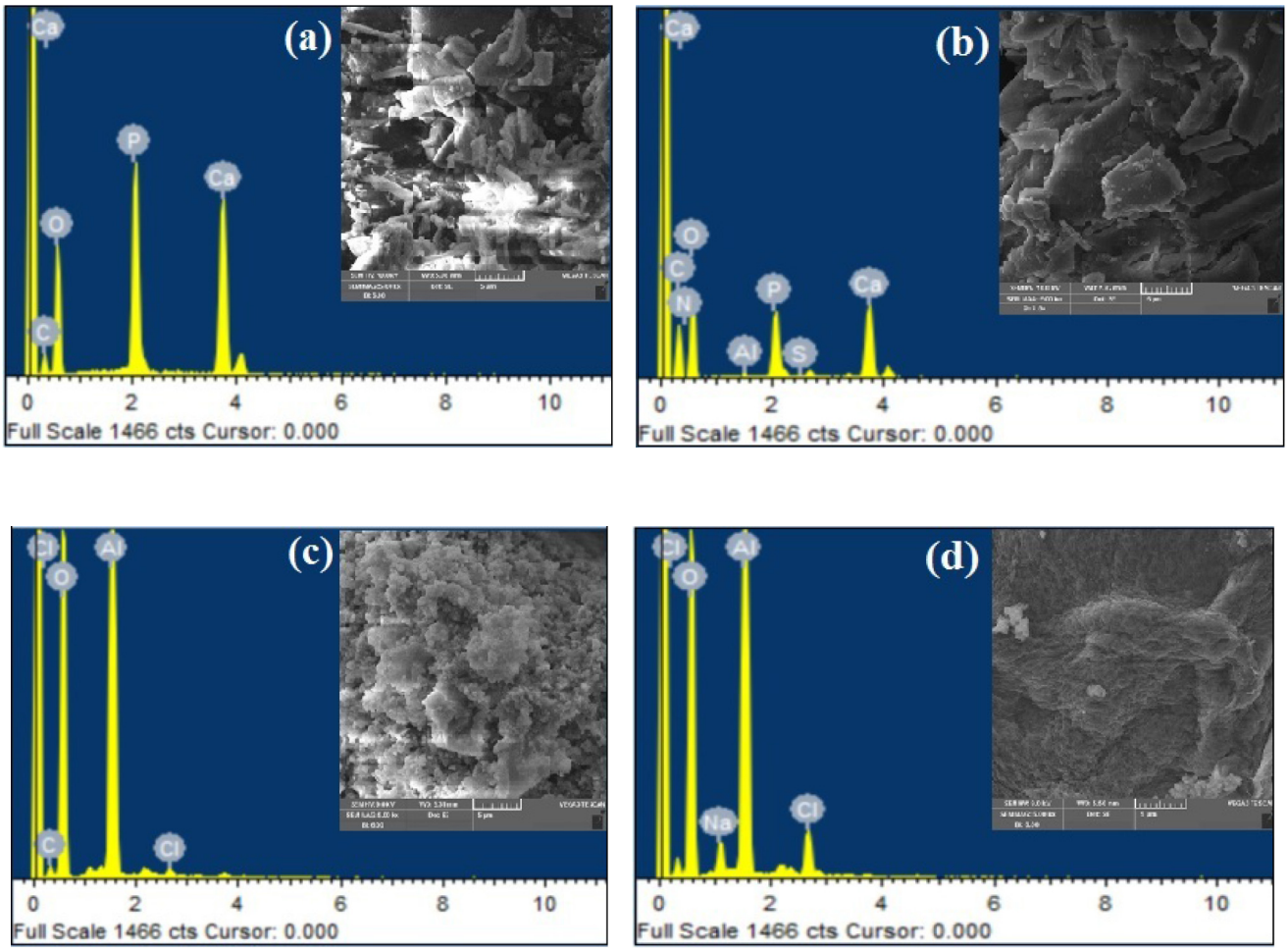

Fig. 4. SEM-EDX of (a) Unloaded biomass pellets (b) Loaded biomass pellets (c) Unloaded Al Flocks (d) Loaded Al Flocks.

(Fig. 5) showed that the lowest decolorization efficiency of 34.01% was achieved in case of the only BS while the maximum removal efficiency of 99.9% was obtained in case of (EC/BS) coupled process after 60 min treatment. The decolourization efficiency achieved after 20 min operation for the various processes were, BS 19.9%, EC 78.29%, EC/BS 99.56% respectively. The EC/BS coupled process was found to be the most efficient among the studied processes to decolorize the RR-241 solution in shorter time periods with a lower current density requirement. The efficiency of the EC/BS coupled process lies in the synergistic mechanisms taking place simultaneously in the reactor, like BS providing sorption sites for dye molecules, EC causing the dye abatement by electro-generated flocs. Furthermore, the parametric studies were performed on EC/BS coupled process.

Table 1
EDX elemental composition (weight %) of biosorbent pellets and Al Flocks

Element	C	O	Ca	P	Al	Cl
Unloaded biosorbent pellets	13.26	54.04	18.16	14.54	–	–
RR-241 loaded biosorbent pellets	25.81	50.26	9.4	5.75	–	–
Unloaded Al Flocks	7.24	57.90	–	–	30.86	0.49
RR-241 loaded Al Flocks	7.40	57.49	–	–	32.68	2.43

3.3. Effect of current density

The current density affects the EC process reaction rate by controlling the metal ions concentration, coagulant production, rate, and size of bubbles formed thereby inducing mass transfer and mixing in the aqueous solution [29–31]. For the electrochemical reactions, the reaction rate is linearly related to the applied current density [15]. The three current densities of 15.49 mA/cm^2, 21.7 mA/cm^2, and 32.03 mA/cm^2 were applied to evaluate the RR-241 decolorization in EC/BS coupled process. The experimental results represented in Fig. 6, revealed a positive influence of applied current density on decolorization efficiency. The decolorization efficiencies of 89.38%, 99.56% and 99.9% were achieved at applied current densities of 15.49 mA/cm^2, 21.7 mA/cm^2 and 32.03 mA/cm^2 after 20 min. The increased removal effi-

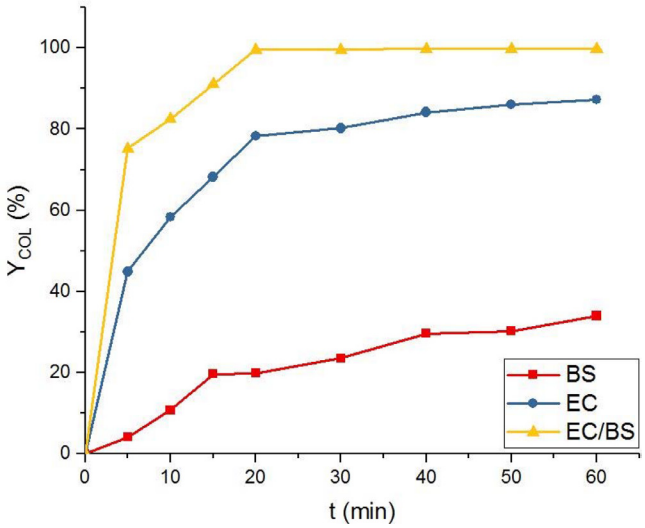

Fig. 5. Decolorization efficiency as a function of different processes (C_o (RR-241) = 50 mg/L; j = 21.7 mA/cm^2; pH = 7; Biosorbent dosage = 8 g/L; Bucket rotational speed = 40 rpm).

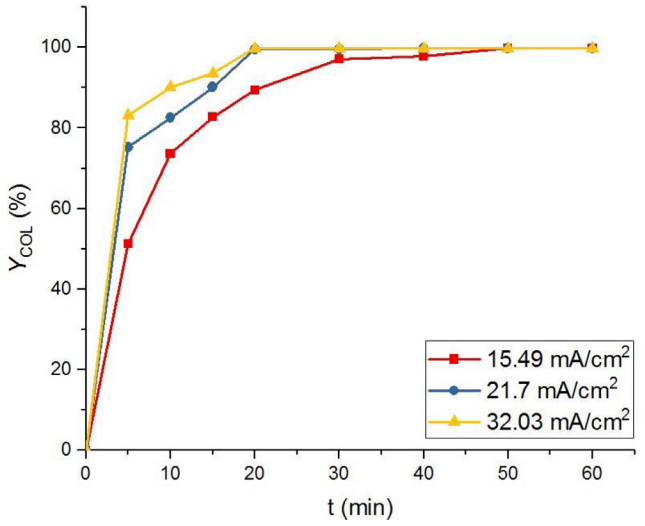

Fig. 6. Effect of current density on decolorization efficiency (C_o (RR-241) =50 mg/L; pH = 7; Biosorbent dosage = 8 g/L; Bucket rotational speed = 40 rpm).

ciency at higher current density may be because at high current density, the rate of bubble generation increases while the size of bubble decreases, which facilitates the pollutant separation process [11]. By enhancing the current density, the anodic oxidation of aluminum plates is enhanced generating more Al^{3+} ions that lead to increase in the concentration of metal hydroxide coagulants $M(OH)_n$ that forms more flocs for dye entrapment [32].

The economics of the EC depends on the applied current density as a higher current density increases the operational cost by enhanced electrode and power consumption but reduces the required treatment time and the capital cost by reduction in reactor size, therefore the optimum current density must be applied as excess may cause the dissipation of electric energy into heat energy thereby increasing the wastewater temperature and thus making the process uneconomical [15]. At higher current density, the temperature of the solution rises thereby enhancing the sorption efficiency by inducing more mass transfer due to a reduction in solution viscosity and kinetic energy enhancement increasing the sorbent-sorbate collision frequency [33].

3.4. Effect of pH

pH is the primary parameter that controls the efficiency of the EC process by augmenting the generation of various monomeric and polymeric metal hydroxides in solution which are strongly solution pH dependent [29,34]. The pH effect was assessed by altering pH in the range 5–9. The obtained results, shown in Fig. 7, revealed that the neutral pH 7 was most suitable for the RR-241 abatement with the highest decolorization efficiency. It was observed that the decolorization efficiency enhanced from 95.5% to 99.9% with pH increase from pH 5 to pH 7 and then decreased to 89.7% at pH 9 after 60 min of treatment. The decolorization efficiencies of 92.56%, 99.56%, and 87.64% were achieved at pH 5, 7 and 9 respectively after 20 min. The highest efficiency at pH 7 can be ascribed as at neutral pH, the formed $Al(OH)_3$ has the minimum solubility which precipitates and traps the dye colloidal species by adsorption as dominant phenomena which are then separated from the solution by H_2 and air flotation at a faster rate to the surface [29,35]. At acidic pH, the Al^{3+} ions are the dominant species and various monomeric and polymeric aluminum hydroxide complexes are generated with the rise in the pH, which are finally transformed into the amorphous solid $Al(OH)_3$ that acts as coagulant to cause charge neutralization and adsorption of pollutant while at alkaline pH, $Al(OH)_4^-$ is the main species which are not effective for adsorption due to high solubility and cause repulsion of anionic dye molecules thereby the decolorization capacity is diminished and decrease in $Al(OH)_3$ occurs [13,32].

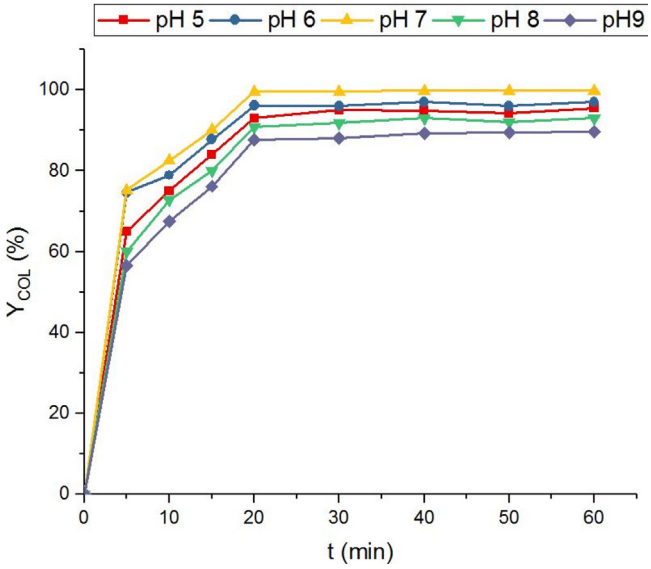

Fig. 7. Effect of pH on decolorization efficiency (C_o (RR-241) =50 mg/L; j = 21.7 mA/cm^2; Biosorbent dosage = 8 g/L; Bucket rotational speed = 40 rpm).

$$Al(OH)_3 + OH^- \rightleftarrows Al(OH)_4^- \quad (14)$$

When pH is lower than 6, various cationic hydrolysis species are formed [$Al(OH)_2^+$, $Al(OH)^{2+}$, $Al_6(OH)_{15}^{3+}$, $Al_8(OH)_{20}^{7+}$, $Al_{13}(OH)_{34}^{5+}$], that destabilizes the anionic dye by charge neutralization due to the opposite charges. The lowest solubility of [0.03 mg Al/L] exists at pH 6.3 and rises when the solution becomes alkaline or acidic thereby favoring the dye coagulation. The results revealed the role of $Al(OH)_3$ as a superior coagulant species in the E-C process as described by various researchers [26,36,37].

3.5. Effect of biosorbent dosage

The biosorbent dosage effect on the decolorization by EC/BS coupled process was studied and Fig. 8 represents the experimental results obtained that compare the process with no biosorbent and 4, 8 and 12 g/L biosorbent dosage. The removal efficiencies of 87.27%, 94.11%, 99.56%, and 99.9% were obtained after 20 min by loading biosorbent dosage of 0 g/L, 4 g/L, 8 g/L and 12 g/L respectively. The results revealed enhancement in dye removal efficiency and reduction in the required treatment time with biosorbent dosage. The high biosorbent dosage provides increased sorption sites for the dye molecules and high surface area [27,38,39] that increases decolorization efficiency.

3.8. Effect of initial RR-241 concentration

The influence of initial RR-241 concentration on decolorization efficiency was assessed at 20 mg/L, 50 mg/L, and 80 mg/L and the obtained results are given in Fig. 9. A reduction in the decolorization efficiency was observed with the rise in the RR-241 concentration. The decolorization efficiencies of 99.9%, 99.56% and 91.75% were achieved with 20 mg/L, 50 mg/L and 80 mg/L RR-241 initial concentration respectively after 20 min. At a specific current density, a fixed amount of metal ions is produced in the reactor that leads to the formation of coagulants which becomes limited when higher dye concentration is used and also a specific biosorbent dosage provides a fixed number of sorption sites for the contaminant. Consequently,

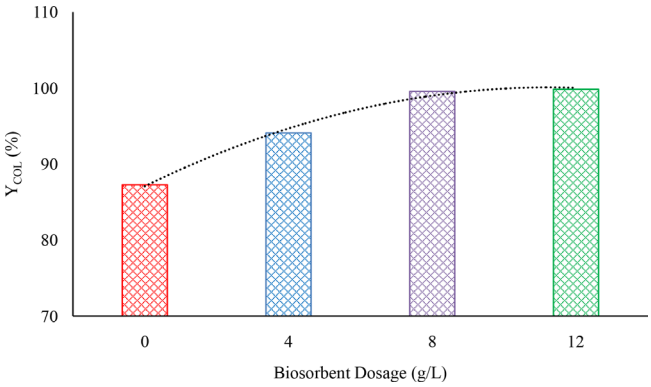

Fig. 8. Effect of biosorbent dosage on decolorization efficiency (C_o (RR-241) = 50 mg/L; j = 21.7 mA/cm^2; pH = 7; Bucket rotational speed = 40 rpm, Time = 20 min).

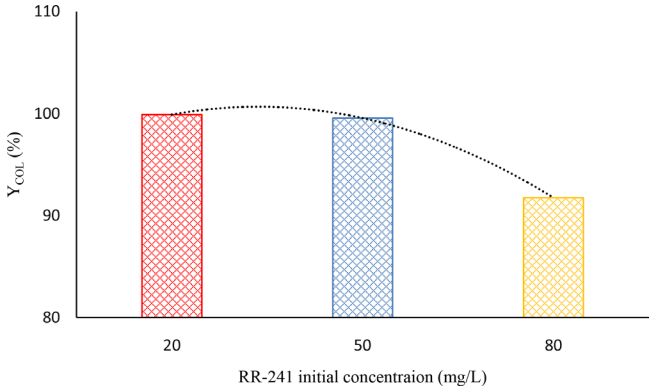

Fig. 9. Effect of RR-241 initial concentration on decolorization efficiency (j = 21.7 mA/cm^2; pH = 7; Biosorbent dosage = 8 g/L; Bucket rotational speed = 40 rpm).

with a rise in the RR-241 concentration, the treatment time to achieve maximum dye removal increases due to a limited number of aluminum hydroxide coagulants produced at the start of the reaction and increases continuously with time [10,40,41].

3.9. Decolorization kinetics

The linear plot of 1st order and 2nd order models are shown in Fig. 10 and Table 2 gives the kinetic parameter values for the processes. The first order model was applied in two phases for (Fig. 10), the initial transition phase (0–20 min) and the settling phase (20–60 min). The experimental results gave the good fit to the first order kinetics. At optimum values, the determined value of rate constant K_1 was 0.105 (min^{-1}) with an R^2 value of 0.988 (Table 2).

3.10. Cost analysis

The operational cost (OC) of hybrid reactor for the treatment of RR-241 was determined based on the main cost components of electrical energy and electrodes consumption.

$$OC = a \times SEEC + b \times UMC \quad (15)$$

OC is the operational cost ($/kg dye), a is the electric energy cost ($/kWh), SEEC is the specific electrical energy consumption (kWh/kg dye), b is the aluminum cost ($/kg) and UMC is the unit electrode material consumption (kg/kg dye). The local electric energy cost was ($ 0.11/kWh), the aluminum cost in the local market was (2.27 $/kg). At optimum conditions, the SEEC was 1.7 kWh/kg dye, and UMC was 0.053 kg/kg dye, the determined OC was 0.307 $/kg dye.

4. Conclusions

The new (EC/BS) hybrid reactor performed efficiently and resulted in complete decolorization of RR-241 aqueous solution and with lower energy requirement and operational cost. At optimum conditions, color removal efficiency of 99.56% was obtained after 20 min at current density

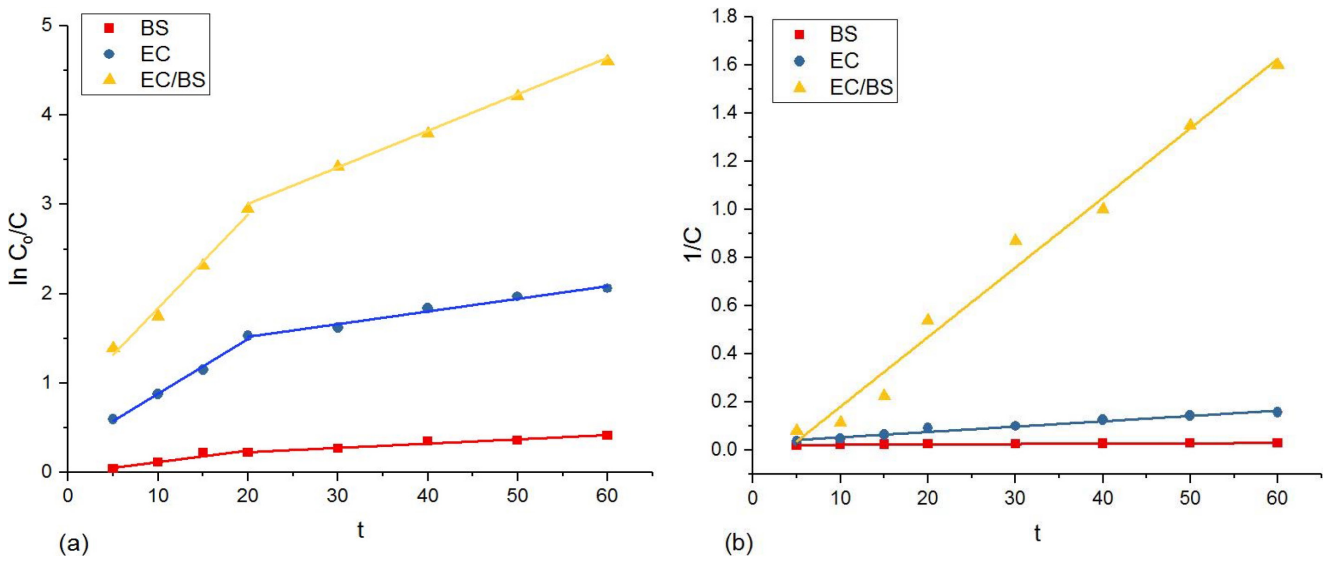

Fig. 10. The kinetic plots of RR-241 decolorization (a) first order (b) second order models.

Table 2
Values of kinetic model parameters for RR-241 decolorization

Process	First order				Second Order		
	BS	EC	EC/BS		BS	EC	EC/BS
1st phase	K_1 (1/min)	0.013	0.061	0.105	K_2 (L/mg·min)	0.0015	0.0022	0.029
	R^2	0.952	0.989	0.988	R^2	0.908	0.964	0.982
2nd phase	K_1 (1/min)	0.005	0.0142	0.041				
	R^2	0.978	0.970	0.983				

21.7 mA/cm^2, pH 7, biosorbent dosage 8 g/L, and dye concentration 50 mg/L with specific electrical energy consumption of 1.7 kWh/kg dye, and operational cost of 0.307 $/kg dye. The decolorization followed first order kinetics with K_1 = 0.105 min^{-1}. The results indicate the potential of electrocoagulation/biosorption (EC/BS) coupled hybrid reactor for the effective treatment of colored effluents.

Acknowledgment

The financial support for the research work (ORIC/100-ASRB/1977) granted by the UET Lahore Pakistan is thankfully acknowledged.

References

[1] F.A.K. Hendaoui, I.B. Rayana, R.B. Amar, F. Darragi, M. Trabelsi-Ayadi, Real indigo dyeing effluent decontamination using continuous electro coagulation cell: Study and optimization using response surface methodology, Process Saf. Environ., 116 (2018) 578–589.
[2] T.-S.C.G. Han, M. Weber, C. Maletzko, Low-pressure nanofiltration hollow fiber membranes for effective fractionation of dyes and inorganic salts in textile wastewater, Environ. Sci. Technol., 52 (2018) 3676–3684.
[3] J.P.K.P. Kaur, V.K. Sangal, Electro catalytic oxidative treatment of real textile wastewater in continuous reactor: Degradation pathway and disposability study, J. Hazard. Mater., 346 (2018) 242–252.
[4] N.F.F. Javed, A. Ikhlaq, M. Kazmi, S.W. Ahmad, H.M.S. Munir, Biosorption potential of Sapindus mukorossi dead leaves as a novel biosorbent for the treatment of Reactive Red 241 in aqueous solution, Desal. Water Treat., 137 (2019) 345–357.
[5] M.K.A. Ikhlaq, F. Javed, H. Fatima, A. Akram, S. Asif, UV/H_2O_2/iron loaded rice husk ash based advanced oxidation process for the removal of safranin in wastewater, Desal. Water Treat., 126 (2018) 306–313.
[6] G.K.K.R.M. Sarvajith, Y.V. Nancharaiah, Textile dye biodecolourization and ammonium removal over nitrite in aerobic granular sludge sequencing batch reactors, J. Hazard. Mater., 342 (2018) 536–543.
[7] E.L.B.N. R.P.F. Melo, S.K.S. Nunes, T.N. Castro Dantas, A.A. Dantas Neto, Removal of reactive blue 14 dye using micellar solubilization followed by ionic flocculation of surfactants, Sep. Purif. Technol., 191 (2018) 161–166.
[8] D.K.M.M. Momeni, F. Abbasi, S. Ghanbarian, Using chitosan/CHPATC as coagulant to remove color and turbidity of industrial wastewater: Optimization through RSM design, J. Environ. Manage., 211 (2018) 347–355.
[9] J.L.S. Cotillas, P. Cañizares, D. Clematis, G. Cerisola, M.A. Rodrigo, M. Panizza, Removal of procion red MX-5B dye from wastewater by conductive-diamond electrochemical oxidation, Electrochim. Acta, 263 (2018) 1–7.
[10] N.K.A.E.S.Z. El-Ashtoukhy, M.M. Abd El-Latif, D.G. Bassyouni, H.A. Hamad, New insights into the anodic oxidation and electro coagulation using a self-gas stirred reactor: A comparative study for synthetic C.I Reactive Violet 2 wastewater, J. Clean. Prod., 167 (2017) 432–446.
[11] Ü.B.O.Y. Yavuz, Treatment of industrial estate wastewater by the application of electro coagulation process using iron electrodes, J. Environ. Manage., 207 (2018) 151–158.

[12] M.A.-S.Z. Al-Qodah, K. Bani-Melhem, E. Assirey, M.A. Yahya, A. Al-Shawabkeh, Free radical-assisted electro coagulation processes for wastewater treatment, Environ. Chem. Lett., 16 (2018) 695–714.
[13] P.N.P.P. Sakthisharmila, P. Manikandan, Removal of benzidine based textile dye using different metal hydroxides generated in situ electrochemical treatment-A comparative study, J. Clean. Prod., 172 (2018) 2206–2215.
[14] B.M.B. Khemila, A. Chouder, R. Zidelkhir, J.-P. Leclerc, F. Lapicque, Removal of a textile dye using photo voltaic electro coagulation, Sustain. Chem. Pharm., 7 (2018) 27–35.
[15] D.B.H. Hamad, E.S. El-Ashtoukhy, N. Amin, M. Abd El-Latif, Electro catalytic degradation and minimization of specific energy consumption of synthetic azo dye from wastewater by anodic oxidation process with an emphasis on enhancing economic efficiency and reaction mechanism, Ecotoxicol. Environ. Saf., 148 (2018) 201–512.
[16] G.K.S.C. Srikantan, S. Srivastava, Effect of light on the kinetics and equilibrium of the textile dye (Reactive Red 120) adsorption by Helianthus annuus hairy roots, Bioresour. Technol., 257 (2018) 84–91.
[17] Z.W.J. Liu, H. Li, C. Hu, P. Raymer, Q. Huang, Effect of solid state fermentation of peanut shell on its dye adsorption performance, Bioresour. Technol., 249 (2018) 307–314.
[18] F.S.T.G.M.D.F. R.A. Fideles, O.F.H. Adarme, L.H.M. da Silva, L. F. Gil, L.V.A. Gurgel, Trimellitated sugarcane bagasse: A versatile adsorbent for removal of cationic dyes from aqueous solution. Part I: Batch adsorption in a monocomponent system, J. Colloid Interface Sci., 515 (2018) 172–188.
[19] M. Kaya, Evaluation of a novel woody waste obtained from tea tree sawdust as an adsorbent for dye removal, Wood Sci. Technol., 52 (2017) 245–260.
[20] V.V.O. Sacco, M. Matarangolo, ZnO supported on zeolite pellets as efficient catalytic system for the removal of caffeine by adsorption and photo catalysis, Sep. Purif. Technol., 193 (2018) 303–310.
[21] J.K.B.M. Dutta, Fixed-bed column study for the adsorptive removal of acid fuchsin using carbon–alumina composite pellet, Int. J. Environ. Sci. Technol., 11 (2013) 87–96.
[22] E.S.F. Asjadi, I. Mobasherpour, Removal of reactive red 141 dye from aqueous solution by titanium hydroxyapatite pellets, J. Dispers. Sci. Technol., 37 (2015) 14–22.
[23] K.Y.F.I. Hai, K. Fukushi, Hybrid treatment systems for dye wastewater, Crit. Rev. Environ. Sci. Technol., 37 (2007) 315–377.
[24] T.P.-S.J. Castañeda-Díaz, E. Gutiérrez-Segura, A. Colín-Cruz, Electro coagulation-adsorption to remove anionic and cationic dyes from aqueous solution by PV-energy, J. Chem., 2017 (2017) 1–14.
[25] L.W.L.C.X.-H. Su, T.T. Teng, Y.S. Wong, Combination and hybridisation of treatments in dye wastewater treatment: A review, J. Environ. Chem. Eng., 4 (2016) 3618–3631.
[26] J.H.H.P. de Carvalho, M. Zhao, G. Liu, L. Dong, X. Liu, Improvement of methylene blue removal by electro coagulation/banana peel adsorption coupling in a batch system, Alexandria Eng. J., 54 (2015) 777–786.
[27] J.N.X. Wang, S. Pang, Y. Li, Removal of malachite green from aqueous solutions by electro coagulation/peanut shell adsorption coupling in a batch system, Water Sci. Technol., 75 (2017) 1830–1838.
[28] A.E.K.M. Elazzouzi, K. Haboubi, M.S. Elyoubi, A novel electro coagulation process using insulated edges of Al electrodes for enhancement of urban wastewater treatment: Techno-economic study, Process Saf. Environ., 116 (2018) 506–515.
[29] N.F.A.G. Khorram, Treatment of textile dyeing factory wastewater by electro coagulation with low sludge settling time: Optimization of operating parameters by RSM, J. Environ. Chem. Eng., 6 (2018) 635–642.
[30] V.D.S.M.A. Ubale, Experimental study on electro coagulation of textile wastewater by continuous horizontal flow through aluminum baffles, Korean J. Chem. Eng., 34 (2017) 1044–1050.
[31] F.G.-D.P. Durango-Usuga, R. Mosteo, M.V. Vazquez, G. Penuela, R.A. Torres-Palma, Experimental design approach applied to the elimination of crystal violet in water by electro coagulation with Fe or Al electrodes, J. Hazard. Mater., 179 (2010) 120–126.
[32] R.C.M.A.S. Fajardo, D.R. Silva, C.A. Martínez-Huitle, R.M. Quinta-Ferreira, Dye waste waters treatment using batch and recirculation flow electro coagulation systems, J. Electroanal. Chem., 801 (2017) 30–37.
[33] B.C.M.S. Secula, T.F. de Oliveira, O. Chedeville, H. Fauduet, Removal of acid dye from aqueous solutions by electro coagulation/GAC adsorption coupling: Kinetics and electrical operating costs, J. Taiwan. Inst. Chem. Eng., 43 (2012) 767–775.
[34] M.K.P.I. Omwene, Treatment of domestic wastewater phosphate by electro coagulation using Fe and Al electrodes: A comparative study, Process Saf. Environ., 116 (2018) 34–51.
[35] M.K.A. Ikhlaq, F. Javed, K.S. Joya, F. Anwar, Combined catalytic ozonation and electro flocculation process for the removal of basic yellow 28 in wastewater, Desal. Water Treat., 127 (2018) 354–363.
[36] H.R.V.J.B. Parsa, A.R. Soleymani, M. Abbasi, Removal of acid brown 14 in aqueous media by electrocoagulation: Optimization parameters and minimizing of energy consumption, Desalination, 278 (2011) 295–302.
[37] Z.Z.S.C.A.S. Naje, S.A. Abbas, Treatment performance of textile wastewater using electro coagulation (EC) process under combined electrical connection of electrodes, Int. J. Electrochem. Sci., (2015) 5924–5941.
[38] M.M.M. Khedher, H.K. El-Etriby, Enhancement of electro coagulation process for dye removal using powdered residuals from water purification plants (PRWPP), Water Air Soil Pollut., 228 (2017).
[39] M.M.B.B. Naraghi, R. Amiri, A. Dorost, H. Biglari, Removal of Reactive Black 5 dye from aqueous solutions by coupled electro coagulation and bio-adsorbent process, Electron. Physician., 10 (2018) 7086–7094.
[40] S.H.R. Khosravi, M. Fazlzadeh, Decolorization of AR18 dye solution by electro coagulation: sludge production and electrode loss in different current densities, Desal. Water Treat., 57 (2015) 14656–14664.
[41] M.G.A. Dalvand, A. Joneidi, N.M. Mahmoodi, Dye removal, energy consumption and operating cost of electro coagulation of textile wastewater as a clean process, CLEAN-Soil Air Water, 39 (2011) 665–672.